The 5th TSME International Conference on Mechanical Engineering
17-19 December 2014, The Empress, Chiang Mai
2014 TSME-ICoME ASEAN AND BEYOND

DRC-003

Quantitative Feedback Control of a Diesel Engine Throttle

Withit Chatlatanagulchai[1,*] and Surarerk Meeudompong[1]

[1] Control of Robot and Vibration Laboratory, Department of Mechanical Engineering, Faculty of Engineering, Kasetsart University, 50 Phahonyothin Rd., Chatuchak, Bangkok, 10900

*Corresponding Author: fengwtc@ku.ac.th, Tel. +66(0) 2797-0999 ext. 1803, 1804, Fax. +66(0) 2579-4576

Abstract

Accurate control of Diesel engine throttle is vital to Diesel engine performance and emission. Engine aging and varying operating conditions require the controller to be robust or adaptive. Existing works, such as adaptive, sliding mode, backstepping, and feedback linearization controls, either are complicated or may require some impractical assumptions. In this paper, for the very first time, quantitative feedback control is applied to the throttle. This type of control explicitly considers all possible plant model variations while ensures that the closed-loop system meets various frequency-domain specifications such as stability, tracking, and disturbance rejection. Experimental results have shown that the throttle can track its wide-range reference input well even under the presence of large power supply variation and ground vibration.

Keywords*:* Quantitative feedback; Throttle; Hysteresis; Disturbance rejection.

1. Introduction

In Diesel engine, throttle is placed after turbocharger and intercooler and before intake manifold. Together with exhausted gas recirculation (EGR) valve and variable geometry turbine (VGT), throttle actuates two important quantities in the air path: the mass air flow (MAF) and manifold absolute pressure (MAP). Therefore, accurate control of throttle position is vital to engine performance and emission.

Control design for throttle position usually performs on a fixed and linear throttle mathematical model. However, the throttle characteristic is not fixed, during engine operation, supply voltage, either from battery or generator, and engine temperature change with time. Production deviations among batches as well as engine aging also exist. Moreover, the throttle characteristic is not linear, hard nonlinearities such as deadzone and hysteresis exist due to friction and actuator design. Therefore, control design using a fixed and linear throttle model may have an unexpected poor performance.

Existing works that deal with this time-varying and nonlinear throttle system include adaptive [1], intelligent system [2] – [4], sliding mode [5], [6], time-optimal [7],and nonlinear controls such as back-stepping [8] and feedback linearization [9]. Still, besides being complicated, they may require some impractical assumptions such as

persistently exciting input or invertible plant model.

In this paper, for the very first time, we have applied quantitative feedback control to throttle. The controller is based on quantitative feedback theory (QFT) introduced by [10]. The design method quantitatively ensures that all specifications from tracking to disturbance and noise rejections are met for all plant models in the uncertain-plant set. The resulting controllers are simply a continuous-time pre-filter and a feedback controller that can be readily implemented.

Several experiments were conducted. First, the throttle was allowed to follow a wide range of reference input from 0 to 80 opening percentages, while the supply voltage changes from 10 to 14 volts. Second, the throttle was placed in a real truck, which was driven around, while the throttle tried to track a stair-case reference. This is to test the disturbance rejection performance of the control system. Third, two time-domain signals were given as lower and upper bounds of the output. This experiment is used to demonstrate that the controlled output stays within pre-specified bounds. Fourth, a hysteresis compensation was used to improve transient response of the throttle.

Experimental results confirm that the control system meets all the pre-specified specifications when the throttle is operated in a wide range, the power supply varies from 10 to 14 volts, and there is ground vibration.

This paper is organized in this way. Section 2 introduces the Diesel engine throttle and its system identifications. Section 3 contains design of the quantitative feedback controller and simulation results. Section 4 has the experimental results, followed by conclusions in Section 5.

2. Diesel Engine Throttle

Fig. 1 depicts the Diesel engine throttle used in our experiment. A DC motor needs 12V DC power supply and a PWM signal with varying duty cycle to move the throttle plate. A potentiometer measures the opening of the throttle plate as an analog signal. Arduino Mega 2560 microcontroller board, together with Matlab and Simulink toolboxes, are used as control hardware and software.

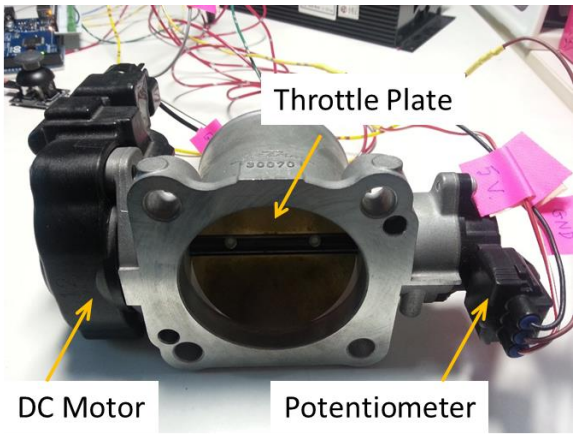

Fig. 1 The Diesel engine throttle used in the experiment.

2.1 Static curve

The duty cycle of the PWM input signal is an 8-bit integer representing values from 0 – 255. These values are recorded as control input u.

The corresponding analog signal from the potentiometer is a 10-bit integer representing values from 0 – 1023. After calibration, these numbers are converted to 0 – 100 opening percentage. The opening percentage is recorded as plant output y.

In creating a static curve, u was slowly given as a triangular-pulse signal from 60 to 200 *ADC*

and back to 60 *ADC* in 120 seconds. y was then recorded. The static curve, which is a plot between u and y, is given in Fig. 2.

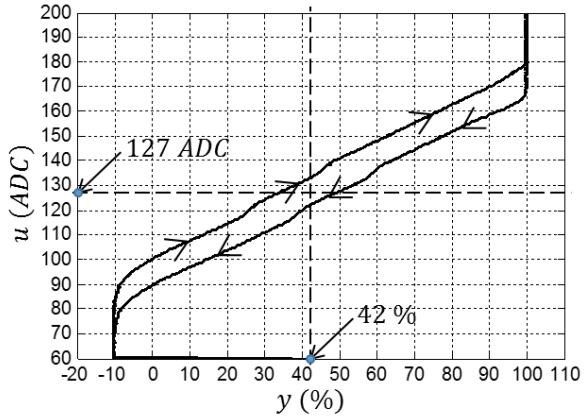

Fig. 2 Throttle static curve.

The static curve is centered around the limp-home position, $y = 42\,\%$, and the middle control input, $u = 127\ ADC$. Hysteresis is evident from the static curve, and there are two obvious nonlinearities around $y = 30$ and $50\,\%$.

2.2 Throttle model

Closed-loop system identification is performed by letting the reference for the opening percentage be a frequency-varying sine wave with frequency range 0.1 – 5 Hz in 30 seconds. A roughly tuned PID controller is used to control the throttle plate. The experiment uses 0.05 seconds sampling time.

The static curve in Fig. 2 appears to be linear in the low range $(0\,\% \le y < 20\,\%)$, medium range $(30\,\% \le y < 50\,\%)$, and high range $(60\,\% \le y < 80\,\%)$, separated by the nonlinearities. Also, in actual engine operation, the supply voltage can vary from 10 to 14 volts.

Table. 1 to Table. 3 contain parameter sets of the throttle model of the form

$$P(s) = \frac{a_1 s + a_2}{s^2 + b_1 s + b_2}$$

when the supply voltage is 10, 12, and 14 volts, respectively.

These parameter values were obtained from repeated closed-loop system identifications of the throttle in Fig. 1.

Table. 1 Parameter sets of the throttle model with 10-volt supply voltage and with varying ranges of reference input.

$60 \le r \le 80\%$: $a_1 = \{9.07, 9.099\}$, $a_2 = \{2.38, 3.279\}$, $b_1 = \{10.32, 10.5\}$, $b_2 = \{5.148, 7.087\}$.
$30 \le r \le 50\%$: $a_1 = \{8.422, 8.433\}$, $a_2 = \{0.638, 0.978\}$, $b_1 = \{9.89, 10.33\}$, $b_2 = \{2.012, 3.08\}$.
$0 \le r \le 20\%$: $a_1 = \{8.52, 8.56\}$, $a_2 = \{0.2174, 0.244\}$, $b_1 = \{10.35, 10.41\}$, $b_2 = \{2.27, 2.54\}$.

Table. 2 Parameter sets of the throttle model with 12-volt supply voltage and with varying ranges of reference input.

$60 \le r \le 80\%$: $a_1 = \{11.83, 12.06\}$, $a_2 = \{1.02, 1.75\}$, $b_1 = \{10.94, 10.99\}$, $b_2 = \{2.17, 3.72\}$.
$30 \le r \le 50\%$: $a_1 = \{11.37, 11.4\}$, $a_2 = \{0.807, 0.83\}$, $b_1 = \{11.49, 11.55\}$, $b_2 = \{2.55, 2.62\}$.
$0 \le r \le 20\%$: $a_1 = \{10.92, 10.96\}$, $a_2 = \{0.35, 0.404\}$, $b_1 = \{11.89, 12.31\}$, $b_2 = \{3.79, 4.35\}$.

Table. 3 Parameter sets of the throttle model with 14-volt supply voltage and with varying ranges of reference input.

$60 \le r \le 80\%$: $a_1 = \{15.4, 15.52\}$, $a_2 = \{0.75, 2.34\}$,

$b_1=\{11.94,12.11\},\ b_2=\{1.57,4.86\}.$
$30\le r\le 50\%$: $a_1=\{15.26,15.33\},\ a_2=\{0.45,0.58\},$ $b_1=\{12.17,12.23\},\ b_2=\{1.432,1.84\}.$
$0\le r\le 20\%$: $a_1=\{13.07,13.15\},\ a_2=\{0.69,0.72\},$ $b_1=\{13.19,13.28\},\ b_2=\{7.67,7.948\}.$

3. Quantitative Feedback Control

From all the plant variations in Table. 1 to Table. 3, minimum and maximum values of each parameter are chosen. Together with their averages, the plant set is given by

$$\left\{\begin{array}{l} P(s)\,|\,a_1=\{8.422,11.971,15.52\},\\ \quad a_2=\{0.2174,1.7482,3.279\},\\ \quad b_1=\{9.89,11.585,13.28\},\\ \quad b_2=\{1.432,4.69,7.948\} \end{array}\right\}, \quad (1)$$

which contains $3^4=81$ plants. The nominal plant $P_0(s)$ is the one with average parameter values.

For each frequency, the plant set can be plotted on the Nichols chart as shown in Fig. 3. The frequencies of interest are 0.5, 1, 2, 4, 8, 10, 15, 30, and 60 *rad/s*. Plant variation region for each frequency is called *plant template*.

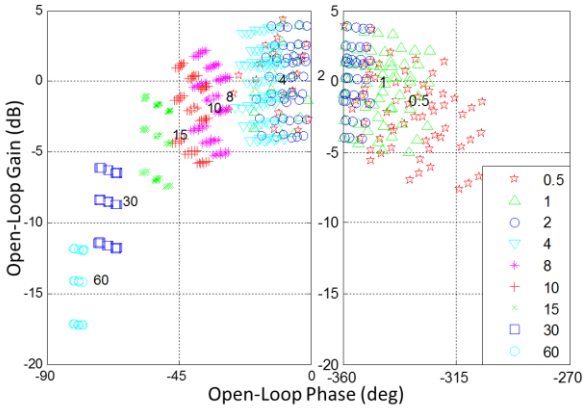

Fig. 3 Plant templates for various frequencies of interest.

In Fig. 4, QFT designs a feedback controller $G(s)$ and a feedforward prefilter $F(s)$ for the closed-loop system to meet various frequency-domain specifications for all plants $P(s)\in\{P\}$ in the plant template. $r, n, e, d_i, u, d_o,$ and y are reference, noise, tracking error, plant-input disturbance, control effort, plant-output disturbance, and output, respectively.

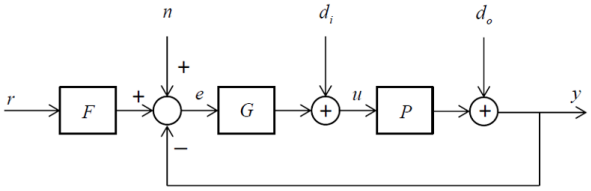

Fig. 4 Closed-loop block diagram of the quantitative feedback control.

Specifications are given as lower or upper bounds of magnitudes of various closed-loop transfer functions relating various signals. Specifications that are of interest in our work will be explored next.

3.1 Stability

In [11], it is shown that a stability specification of the form

$$\left|\frac{y}{n}\right|=\left|\frac{P(j\omega)G(j\omega)}{1+P(j\omega)G(j\omega)}\right|<\delta_s, \quad (2)$$

where δ_s is a small positive number, is equivalent to the gain margin (GM) and phase margin (PM) of

$$GM>20\log\left(\frac{\delta_s+1}{\delta_s}\right)dB,$$
$$PM>2\sin^{-1}\left(\frac{1}{2\delta_s}\right)rad. \quad (3)$$

3.2 Tracking

Tracking specification is given by

$$\alpha \le \left| \frac{P(j\omega)G(j\omega)F(j\omega)}{1+P(j\omega)G(j\omega)} \right| = \left| \frac{y}{r} \right| \le \beta, \quad (4)$$

where α and β are lower and upper bounds. Typically, these bounds can be:

1) Transfer functions, representing systems, having desired transient responses

2) Bode magnitude of the transfer functions, given as frequency-versus-magnitude pairs

3) Two constants close to ones.

It was shown in [11] that $G(s)$ reduces variation from uncertainty so that the magnitude in (4) is narrower than the bounds whereas $F(s)$ shifts the magnitude to be within bounds.

3.3 Plant-output disturbance rejection

This specification is of the form

$$\left| \frac{y}{d_o} \right| = \left| \frac{1}{1+P(j\omega)G(j\omega)} \right| < \delta_{do}, \quad (5)$$

where δ_{do} is a small constant. Because the throttle is placed in vehicle, which is subject to external vibration from road surface, small δ_{do} ensures appropriate disturbance rejection.

3.4 Other specifications

Other specifications, such as control effort, model matching, and plant-input disturbance rejection, can also be included in the design; however, they do not concern our problem.

3.5 Combining specifications

From the highest natural frequency of the plant model, the cut-off frequency for the closed-loop system is aimed to be around $8\,rad/s$; therefore, the bounds for (4) are chosen as shown in Table. 4.

Table. 4 Bounds for tracking specification.

$\omega(rad/s)$	0.5	1	2	4	8	10
$\beta(dB)$	0	0	0	-0.3	-1.5	-3
$\alpha(dB)$	-0.6	-0.6	-0.8	-1.6	-4	-6

For the stability specification (2), δ_s is chosen as 3 dB, which according to (3) should give $GM > 4.65\,dB$ and $PM > 41.46^{\circ}$. Because, in the experiment, the sampling period is set at 0.05 seconds, which gives a Nyquist frequency of 62.83 rad/s, the stability specification is imposed on the following frequencies: 0.5, 1, 2, 4, 8, 10, 15, 30, and 60 rad/s.

For the plant-output disturbance rejection specification (5), δ_{do} is chosen as -3 dB, which should give enough attenuation of the ground vibration. Because the ground vibration is usually in lower frequencies, the disturbance rejection specification is imposed on the following frequencies: 0.5, 1, 2, 4, 8, and 10 rad/s.

Using quadratic-form method in [11], the frequency-domain specifications (2), (4), and (5) are converted to bounds on Nichols chart as shown in Fig. 5. Only the worst-case bounds are plotted.

Nominal loop shape $L_0(s) = G(s)P_0(s)$ must be shaped by appending $G(s)$ so that the points on the loop shape lie in the allowable regions of bounds for each frequency. Fig. 5 also shows original loop shape $L_0(s) = G(s)P_0(s)$, $G(s) = 1$.

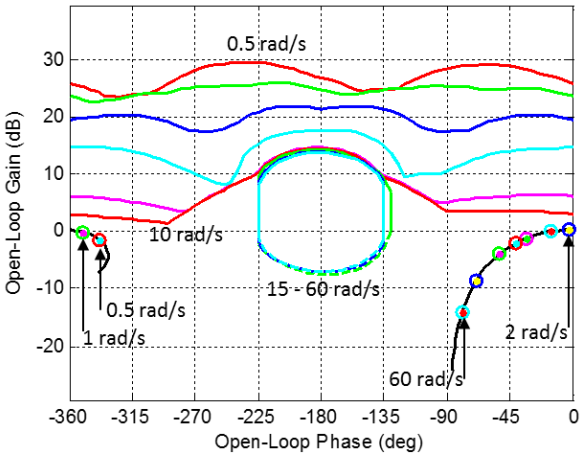

Fig. 5 Bounds on the Nichols chart and original loop shape $L_0(s)=G(s)P_0(s),\ G(s)=1.$

The allowable regions of the tracking, stability, and disturbance rejection specifications are either outside of the ovals or above the lines.

3.6 Loop shaping

$G(s)$ can now be designed to shape the original loop shape. Because the plant is of type 0, for zero steady-state error in following step reference, an integrator s is appended. A lag $(s+11.51)/(s+0.022)$ is added to increase gain; then, a zero $(s+0.068)$ is used to get more phase. A gain of 1.516 then shifts the loop shape upward so that the bound at 0.5 rad/s is satisfied. The final loop shape, using a controller

$$G(s)=\frac{1.516(s+11.51)(s+0.068)}{s(s+0.022)}, \quad (6)$$

is shown in Fig. 6.

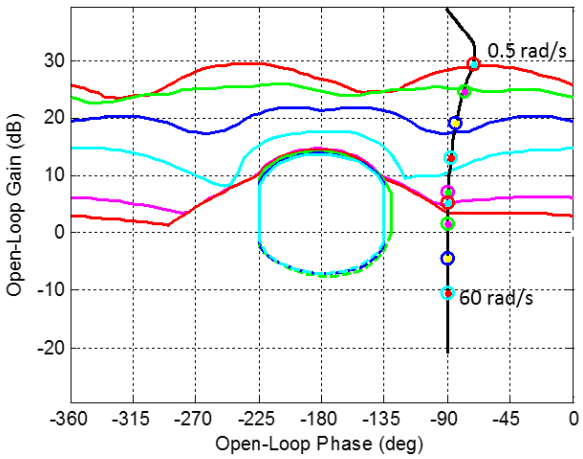

Fig. 6 Bounds on the Nichols chart and final loop shape.

The prefilter $F(s)$ can then be designed to shift the magnitude in (4) to be within bounds. Fig. 7 shows the loop shape of $|PGF/(1+PG)|$ before and after loop shaping. The final $F(s)$ is given by

$$F(s)=\frac{11.3}{(s+11.5)}. \quad (7)$$

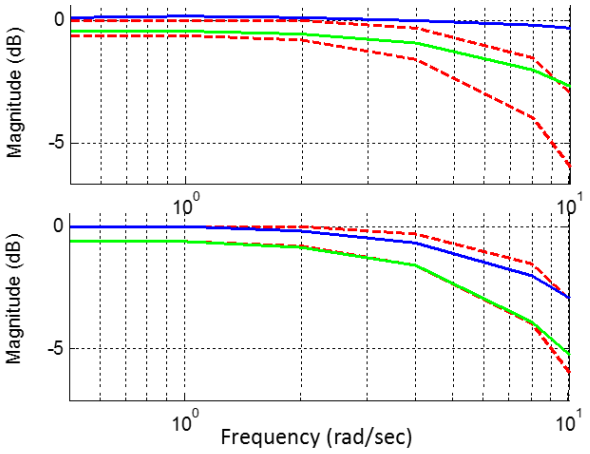

Fig. 7 Closed-loop magnitude $|PGF/(1+PG)|$. (Top) Before shaping. (Bottom) After shaping. Dashed lines are the bounds.

3.7 Simulation results

The system in Fig. 4 is simulated with all 81 plant models in the set (1), the controller (6), and the prefilter (7). In frequency-domain, the Bode magnitude plots of $|PG/(1+PG)|$, $|FPG/(1+PG)|$, and $|1/(1+PG)|$ are given in Fig. 8, where asterisks mark the specification bounds. The results show that the stability (2), tracking (4), and plant-output disturbance rejection (5) specifications are met by all 81 plant models in the set, as was designed for.

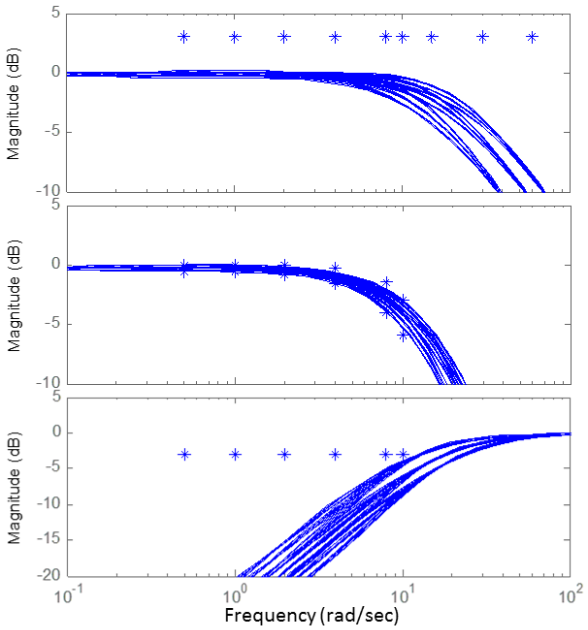

Fig. 8 Simulation results. (Top) $\left|PG/(1+PG)\right|$. (Middle) $\left|FPG/(1+PG)\right|$. (Bottom) $\left|1/(1+PG)\right|$. Asterisks mark corresponding bounds.

4. Experimental Results

4.1 Stair-case reference tracking

This experiment is designed to evaluate the tracking performance of the control system when the supply voltage varies from 10 to 14 volts and when the throttle is operated in a wide range from 0 to 80 opening percentages.

Fig. 9 shows the output y versus the reference input r. The control system can track a wide-range reference well, even under supply voltage variation.

Fig. 10 shows the corresponding control effort u. As expected, the lower the supply voltage, the higher the amplitude of u.

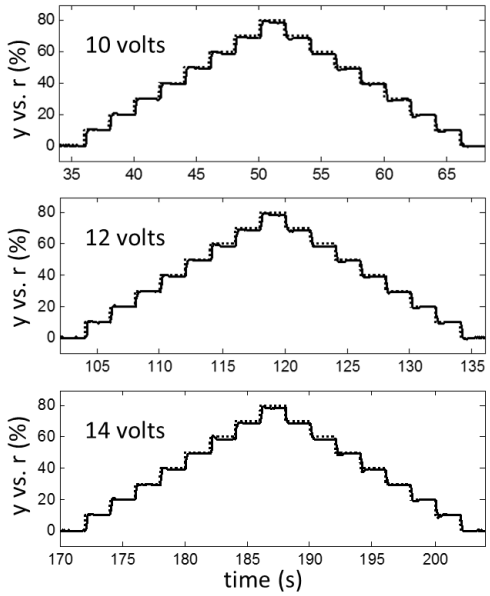

Fig. 9 Tracking performance: (top) with 10 volts, (middle) with 12 volts, and (bottom) with 14 volts supply. Dashed lines are reference input r.

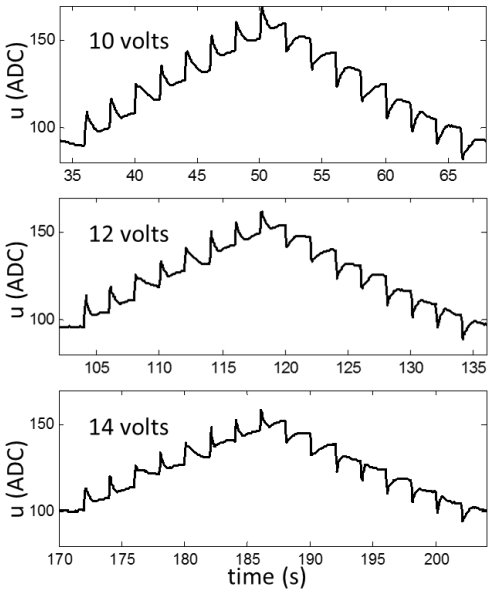

Fig. 10 Control effort: (top) with 10 volts, (middle) with 12 volts, and (bottom) with 14 volts supply.

4.2 Tracking under actual ground vibration

This experiment evaluates the plant-output disturbance rejection performance. The throttle experimental set was installed in an actual Diesel truck. The experiment was run while the truck was driven on an actual road.

Fig. 11 shows the tracking performance with 12 volts supply. It can be seen that the control system can reject the ground vibration well so that it does not affect the tracking performance.

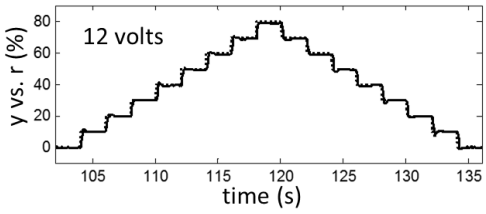

Fig. 11 Tracking performance under ground vibration with 12 volts supply.

4.3 Tracking between bounds

This experiment is designed to show that the output in fact stays between the lower and upper bounds, α and β, during tracking.

To see that, the bounds are changed to two second-order transfer functions:

$$\alpha(s) = 0.95\frac{7^2}{s^2+2(1)(7)s+7^2},$$

$$\beta(s) = 1.05\frac{6.8^2}{s^2+2(0.6)(6.8)s+6.8^2},$$

whose transient responses are desirable.

Control design is repeated because of the change of bounds. The resulting controller and prefilter are given by

$$G(s) = \frac{0.933(s+11.51)(s+0.068)}{s(s+0.022)},$$

$$F(s) = \frac{6.89}{(s+6.74)}.$$

Fig. 12 shows the tracking result. Notice that the higher value of r, the further the bound output y_α from y_β. This is because r is multiplied by the constant bound gains 0.95 and 1.05. The output y (solid line) stays between the bound outputs y_α and y_β (dash-dot lines) for all values of r (dotted line) from 0 to 80 % as it was designed for.

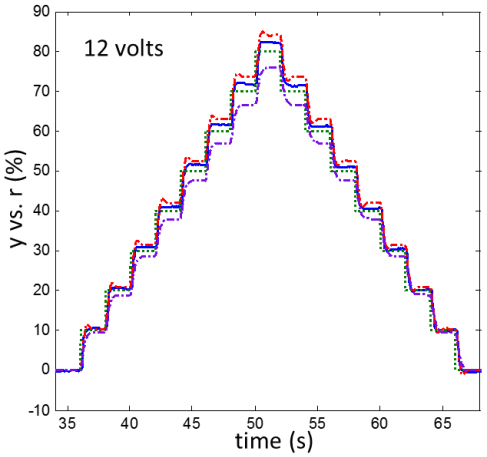

Fig. 12 Tracking between lower and upper bounds. Solid line is y. Dotted line is r. Two dash-dot lines are y_α and y_β.

4.4 Hysteresis compensation

In this experiment, the static curve (Fig. 2) of the throttle is used to compensate for hysteresis. When y increases, 5 ADC is added to the control effort u. When y decreases, 5 ADC is subtracted from the control effort u.

Fig. 13 shows the result of tracking a triangular wave. Transient response is improved with hysteresis compensation.

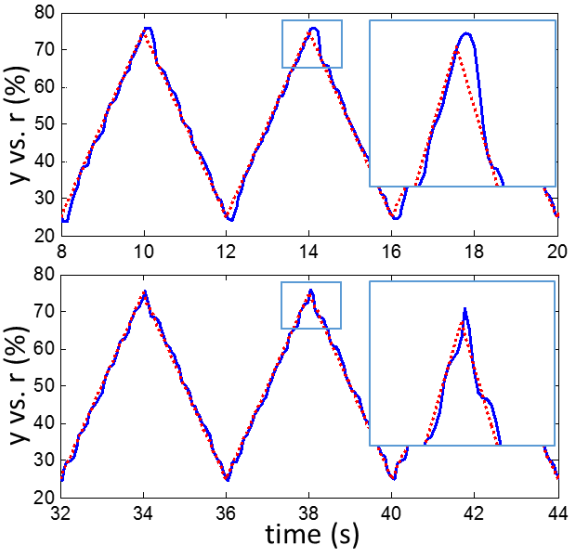

Fig. 13 Tracking performance. (Top) without and (bottom) with hysteresis compensation.

5. Conclusions

For the very first time, we apply quantitative feedback control to a Diesel engine's electronic throttle. The control design explicitly considers plant model uncertainty and various frequency-domain specifications.

The throttle can track its wide-range reference well even under the presence of power supply variation and ground vibration. A hysteresis compensation improves its transient response.

The Diesel engine throttle does not have as strong limp-home effect as in that of the gasoline engine. As a future research, it is interesting to see how the quantitative feedback control performs with the gasoline engine throttle and with a limp-home compensator.

6. References

[1] Pavkovic, D., Deur, J., Jansz, M. and Peric, N. (2006). Adaptive control of automotive electronic throttle, *Control Engineering Practice,* vol. 14, pp. 121 – 136.

[2] Xiaofang, Y., Yaonan, W., Wei, S. and Lianghong, W. (2010). RBF networks-based adaptive inverse model control system for electronic throttle, *IEEE Trans. on Control Systems Tech.,* vol. 18(3), pp. 750 – 756.

[3] Yuan, X., Wang, Y., Wu, L., Zhang, X. and Sun, W. (2010). Neural network based self-learning control strategy for electronic throttle valve, *IEEE Trans. on Vehicular Tech.,* vol. 59(8), pp. 3757 – 3765.

[4] Baric, M., Petrovic, I. and Peric N. (2005). Neural network-based sliding mode control of electronic throttle, *Engineering Applications of Artificial Intelligence,* vol. 18, pp. 951 – 961.

[5] Pan, Y., Ozguner, U. and Dagci, O.H. (2008). Variable-structure control of electronic throttle valve, *IEEE Trans. on Industrial Elec.,* vol. 55(11), pp. 3899 – 3907.

[6] Rossi, C., Tilli, A. and Tonielli, A. (2000). Robust control of a throttle body for drive by wire operation of automotive engines, *IEEE Trans. on Control Systems Tech.,* vol. 8(6), pp. 993 – 1002.

[7] Vasak, M., Baotic, M., Petrovic, I. and Peric, N. (2007). Hybrid theory-based time-optimal control of an electronic throttle, *IEEE Trans. on Industrial Elec.,* vol. 54(3), pp. 1483 – 1494.

[8] Bai, R., Tong, S. and Karimi, H.R. (2013). Modeling and backstepping control of the electronic throttle system, *Mathematical Problems in Engineering,* vol. 2013, 6 pp.

[9] Mercorelli, P. (2009). Robust feedback linearization using an adaptive PD regulator for a sensorless control of a throttle valve, *Mechatronics,* vol. 19, pp. 1334 – 1345.

[10] Horowitz, I. (1959). Fundamental theory of linear feedback control systems, *Trans. IRE on Auto. Control,* vol. 4(3), pp. 5 – 19.

[11] Yaniv, O. (1999). *Quantitative Feedback Design of Linear and Nonlinear Control Systems,* ISBN: 978-0792385295, Springer.